20th IMEKO TC4 International Symposium and
18th International Workshop on ADC Modelling and Testing
Research on Electric and Electronic Measurement for the Economic Upturn
Benevento, Italy, September 15-17, 2014

Synchronization scheme of three terminal MTJ devices

Riccardo Tomasello[1], Mario Carpentieri[2], Giovanni Finocchio[3]

[1]*Department of Computer Science, Modeling, Electronics and System Science, University of Calabria, Rende (CS), Italy.*
[2]*Department of Electrical and Information Engineering, Politecnico of Bari, via E. Orabona 4, I-70125 Bari, Italy.*
[3]*Department of Electronic Engineering, Industrial Chemistry and Engineering, University of Messina, C.da di Dio, I-98166, Messina, Italy.*

***Abstract* –This work deals with a micromagnetic model able to characterize nanoscale oscillators based on three terminal magnetic tunnel junctions. The effect of the spin-transfer torque and the spin-orbit torque are taken into account. Our results predict that the possibility to couple spintronics to spin-orbitronics, and specifically to separate electrically those two torque sources, A scalable synchronization scheme based on the parallel connection of those three terminal devices is proposed.**

I. INTRODUCTION

Synchronization service is commonly used in many contexts, such as to synchronize electrical signals [1], [2] used for triggering of measurement devices or actuators [3], to synchronize clocks [4], [5] for studying dynamics of systems in distributed monitoring or execute scheduled events. The innovative research that we propose regards the synchronization of nanodevices, namely Magnetic Tunnel Junctions (MTJs), in order to generate a unique oscillating signal from many synchronized ones at low power.

Experimental demonstrations of magnetization switching [6], domain wall motion [7] and persistent magnetization precession [8], induced by an in-plane current injection in heavy metal/ferromagnetic/oxide trilayer, have drawn increasing interest to spin torques based on orbital-to-spin momentum transfer (SOT) from Rashba effect and spin-Hall effect (SHE) [9]. Particularly, in the design of the next generation of spintronic devices, together to the advantage to use SOT and especially the SHE (obtaining, in this way, spin-injection without the presence of a ferromagnetic polarizer layer), it will be essential to include the spin-transfer torque (STT) from polarized currents, in order to improve the efficiency and the dynamical properties of those devices.

Here, we study a three terminal device coupling spintronics with spin-orbitronics, which has been introduced by Liu *et al.* [10], [11]. We performed a systematic micromagnetic study of the microwave emission properties (magnetization self-oscillations) driven by the SHE. The three terminal device is composed by a magnetic tunnel junction (MTJ) CoFeB(2)/MgO(1.2)/CoFeB(4)/Ta(5)/Ru(5) (thicknesses in nm) built over a Tantalum (Ta) strip (6000x1200x6 nm^3) [11]. The CoFeB(2) is the free layer of the MTJ, whereas the CoFeB(4) acts as the pinned layer. Fig. 1 shows a detailed sketch of the system, in which a Cartesian coordinate system is introduced, where the *x*-axis is oriented along the larger dimension of the Tantalum strip, the *y*- and *z*-axis are related to its width and thickness respectively. The main advantage to study this system is the possibility to control the injection of two current densities: the in-plane J_{Ta} in the Tantalum strip and the perpendicular J_{MTJ} flowing into the MTJ-stack, achieving an additional degree of freedom in the control of the magnetization dynamics. The main result of this work is a spintronic-spin-orbitronic synchronization scheme which can be used either to improve the properties of the oscillators (linewidth, output power) or to enhance the sensitivity of resonant microwave signal detectors.

II. MICROMAGNETIC MODEL

A self-implemented "state of the art" micromagnetic solver has been used to numerically solve the Landau-Lifshitz-Gilbert equation [12], which includes the STT from a spin-polarized current and the SOT related to the SHE [13]:

$$\frac{d\mathbf{m}}{\gamma_0 M_S dt} = -\frac{1}{(1+\alpha^2)}\mathbf{m}\times\mathbf{h_{EFF}} - \frac{\alpha}{(1+\alpha^2)}\mathbf{m}\times\mathbf{m}\times\mathbf{h_{EFF}}$$
$$-\frac{d_J}{(1+\alpha^2)\gamma_0 M_S}\mathbf{m}\times\mathbf{m}\times\boldsymbol{\sigma} + \frac{\alpha d_J}{(1+\alpha^2)\gamma_0 M_S}\mathbf{m}\times\boldsymbol{\sigma} \qquad (1)$$
$$+\frac{g}{|e|}\frac{|\mu_B| J_{MTJ}}{\gamma_0 \ M_s^2 \ t} g_T(\mathbf{m},\mathbf{m_p}) \ \left[\mathbf{m}\times(\mathbf{m}\times\mathbf{m_p}) - q(V)(\mathbf{m}\times\mathbf{m_p})\right]$$

being $\mathbf{m}$, $\mathbf{h_{EFF}}$ and $\mathbf{m_p}$, the magnetization and the

ISBN-14: 978-92-990073-2-7

effective field of the CoFeB free layer and the magnetization of the polarizer (fixed along the $-y$ direction). α is the Gilbert damping, g is the Landè factor, μ_B is the Bohr magneton, e is the electron charge, γ_0 is the gyromagnetic ratio, M_s is the saturation magnetization and t the thickness of the free layer. $g_T(\mathbf{m},\mathbf{m_p})=\frac{2\eta_T}{1+\eta_T^2\mathbf{m}\cdot\mathbf{m_p}}$ characterizes the angular dependence of the spin-polarization function as computed by Slonczewski [14], [15], η_T is the polarization efficiency. *q(V)* is a function which takes into account the voltage dependence of the field-like torque term in the MTJ up to a maximal value equal to the 25% of the in-plane torque. The coefficient $d_J=\frac{\mu_B\alpha_H}{eM_St}J_{Ta}$, where α_H is the spin Hall angle (ratio between the spin-current J_{SHE} and the J_{Ta}). $\boldsymbol{\sigma}$ is the direction of the J_{SHE} in the Ta-strip. The $\mathbf{h_{EFF}}$ takes into account, as well as the standard micromagnetic energy contributions from external, magnetostatic and exchange field, the Oersted field from both J_{Ta} and J_{MTJ}, the dipolar coupling from the pinned layer. First of all, we carried out preliminary numerical simulations of the same structure studied by Liu *et al.* in Ref. [11], analysing different cross-sections and free layer thicknesses, in order to geometrically optimize the device response in terms of magnetization dynamics. In the following, we present the micromagnetic study for the best geometry configuration to obtain stable states of the magnetization precession. In this case, the dimensions of the ellipse are: w=100 nm along the x-axis and l=300 nm along the y-axis, and thickness t=2 nm. Particularly, we identified a configuration which permits to excite a quasi-uniform mode and to achieve promising results for the injection locking phenomenon driven by a "weak" microwave current (STT) and a fixed bias J_{Ta} (SHE). The physical parameters used in this micromagnetic study are: saturation magnetization M_S=1000x10^{3}A/m, exchange constant A=2.0x10^{-11}J/m, magnetic damping α=0.015, spin-hall angle α_H =-0.15 and spin-polarization η_T =0.66.

III. RESULTS AND DISCUSSIONS

Fig. 1b shows the oscillation frequency as a function of J_{Ta} related to the oscillation of the y-component of the free layer magnetization for two different field amplitudes H_{ext}=30 and 40 mT (J_{MTJ}=0 A/cm^2). The external field is applied with an in-plane angle tilted ϕ=30° with respect to the x-axis of the ellipse. For this thickness, the critical current densities are of the order of 10^8 A/cm^2 and are almost independent on the field amplitude (at least for the simulated values 20-50 mT).

As the field amplitude increases, a decreasing of the current region where coherent magnetization dynamics is observed (e.g. at H_{ext}=40 and 30 mT the range are between -1.65 and -1.95x10^8 A/cm^2 and between -1.38 and -1.97x10^8 A/cm^2 respectively). As expected, the oscillation frequency increases with the amplitude of the external field and its value at the critical current is 3.75 GHz for H_{ext}=30 mT and 4.60 GHz for H_{ext}=40 mT. It exhibits a slightly red-shift (due to the coupling between the phase and the power in those kind of oscillators) as a function of J_{Ta}, indicating the presence of an in-plane oscillation axis.

Fig. 1b shows the oscillation frequency of the main excited mode for a fixed J_{Ta}=-2.13x10^8 A/cm^2 as a function of a bias J_{MTJ}. For positive J_{MTJ}, the oscillation frequency exhibits small variation near 3.75 GHz, while a large frequency tunability around 100 MHz/(10^6 A/cm^2) for negative J_{MTJ} is observed. This result can be explained in the following way. A positive J_{MTJ} acts as an additional positive damping, in fact, for J_{MTJ} larger than 7x10^6 A/cm^2, the microwave emission is switched off. On the contrary, a negative J_{MTJ} acts as a negative damping, showing a significant role in the oscillator frequency.

One of the main properties of spin-torque oscillators (STOs) is the possibility to control the output frequency of the self-oscillation via the injection locking phenomenon [16]. For in-plane magnetized free layer, the injection locking has been observed at

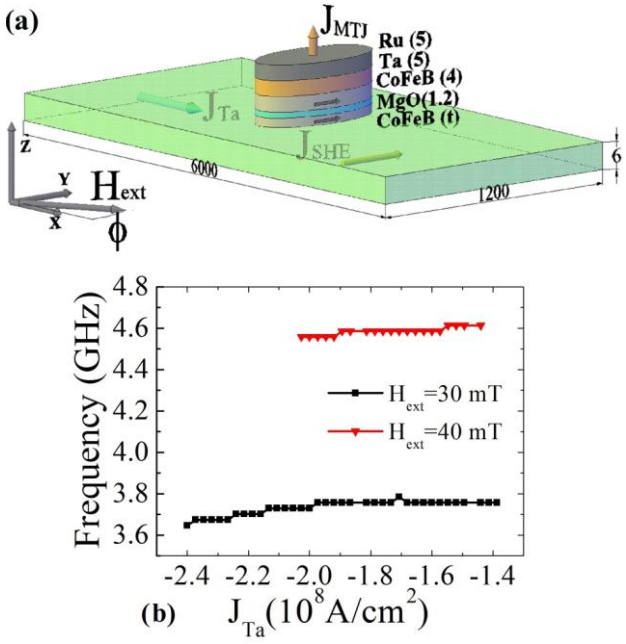

Fig. 1. (a) Schematic representation of the three terminal MTJ device. (b) Oscillation frequency of the magnetization as a function of the J_{Ta} for H_{ext}=40mT (top curve) and H_{ext}=30mT (bottom curve) when the J_{MTJ} is zero.

the 2nd-harmonic (in our case the frequency of the *y*-component of the magnetization). In general, the microwave currents were applied to the same terminal of the bias current. Here, the magnetization precession is driven by the J_{Ta}, while the injection locking is due to a microwave current density $J_{MTJrf} = J_{MAX}\,\mathrm{sen}(2\pi f_{rf} t)$ applied via the third terminal (J_{MAX} and f_{rf} are the amplitude and the microwave frequency). In other words, this system permits to study the non-autonomous behavior of an STO by separating electrically the biasing current from the microwave source. We fixed J_{Ta}=-2.13 x 10^8 A/cm^2 and H_{ext}=30 mT, which corresponds to an oscillation frequency of 3.75GHz. The locking properties have been studied for a J_{MTJrf} with amplitude J_{MAX} from 1 to 4.2x10^6 A/cm^2 at T=0 K and up to 8x10^6 A/cm^2 for T=300 K and a microwave frequency from 3.0 GHz to 8.0 GHz. Fig. 2a summarizes the locking range Δ as a function of J_{MAX}, without and with the thermal fluctuations (T=300 K). For example, at J_{MAX}=2x10^6 A/cm^2, the locking range is Δ=320 MHz, from 3.61 to 3.93 GHz. For current densities up to 4.2x10^6 A/cm^2, the response is qualitatively the same where the Δ increases linearly with J_{MAX}. The thermal field $\mathbf{h}_{\mathrm{th}}$ is considered as an additive term to the effective field, being $\mathbf{h}_{th} = (\xi / M_s)\sqrt{2(\alpha K_B T / \mu_0 \gamma_0 \Delta V\, M_s\, \Delta t)}$, where K_B is the Boltzmann constant, ΔV is the volume of the computational cubic cell, Δt is the simulation time step, T is the temperature of the sample and ξ is random numbers from a Gaussian distribution with zero mean and unit variance.The presence of thermal fluctuations imposes a larger J_{MAX} to reach the same locking region Δ. The different trends of the two curves in Fig. 3a are ascribed to non-isochronous behaviors when the microwave current is high [17]. When the thermal fluctuations are taken into account, such behavior is shown at larger currents. Our results predict locking regions comparable or even larger than the experimental ones for microwave current densities of the same order. In the synchronization region, where the resistance r oscillates at the same frequency ω_S of the microwave source, the signal can be written as $r = R_{<M>,S} + \Delta R_S \sin(\omega_S t + \phi_S)$, being ΔR_S and $R_{<M>,S}$ the amplitude of the oscillating tunnelling magnetoresistive signal and its mean value respectively, and ϕ_S the intrinsic phase shift in the synchronized state [18]. The output voltage v_0 measured on the MTJ is given by:

$$v_0 = \left(R_{<M>,S} + \Delta R_S \sin(\omega_S t + \phi_S)\right) I_{MAX} \sin(\omega_S t) =$$

$$= R_{<M>,S} I_{MAX}\,\mathrm{sen}(\omega_S t) + \frac{\Delta R_S I_{MAX}}{2}\left(\cos(\phi_S) - \cos(2\omega_S t + \phi_S)\right) \quad (2)$$

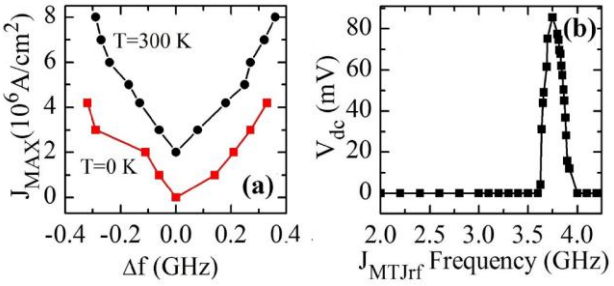

Fig. 3. (a) Arnold tongues showing the locking regions as function of J_{MTJrf} for T=0 K (lower curve) and T=300 K (upper curve) at J_{Ta}=-2.13 x 10^8 A/cm^2. (b) Dc output voltage vs f_{rf} as computed with Eq. 2 for J_{MAX} =2x10^6 A/cm^2. Inset: intrinsic phase shift ϕ_S as function of f_{rf} inside the locking region (J_{MAX} =2x10^6 A/cm^2).

where $I_{MAX} = SJ_{MAX}$ (S is the cross section of the free layer). Together to the microwave signals at $2\omega_S$ and ω_S, that can be used for the design of microwave oscillators, a dc component $0.5\Delta R_S I_{MAX}\cos\phi_S$ is also observed. Fig. 2b shows the dc output voltage as function of the microwave frequency for a J_{MAX}=2x10^6 A/cm^2. A maximum voltage of 80 mV is achieved inside Δ, whereas zero dc voltage is measured outside Δ. The prediction of this large dc voltage makes this system very promising for the design of a next generation of high sensitive resonant microwave signal detectors. The results described above are at the basis of the synchronization scheme discussed below.

Now, we focus our attention on MTJs with different cross sections (MTJ$_1$, MTJ$_2$, and MTJ$_3$) with in plane axes 310 and 100 nm, 300 and 100 nm (same studied above), 290 and 100 nm respectively. Fig. 4 shows a sketch of the proposed synchronization scheme for the three MTJs, but we stress the fact that this system is highly scalable and it can be extended to an array of N-three terminal systems.

The dependence of the oscillation frequency on J_{Ta} in MTJ$_1$ and MTJ$_3$ is similar to the one related to the MTJ$_2$. For a fixed J_{Ta}, the locking range of the three MTJs is of the same order, but centered over a different oscillation frequency. For example, at J_{Ta}=-2.13x10^8 A/cm^2 and J_{MAX}=2.0x10^6 A/cm^2, we achieved for MTJ$_1$ a magnetization precessional frequency f_1=3.62 GHz and Δ$_1$=390 MHz, for MTJ$_2$ f_2=3.75 GHz and Δ$_2$=320 MHz, and for MTJ3 f_3=3.78 GHz and Δ$_3$=310 MHz. The locking ranges are overlapped for a region of 290 MHz, suggesting a possible way to synchronize parallel connected three terminal oscillators.

The magnetization precession is excited by means of the SHE in all the MTJs. The synchronization is achieved via a microwave voltage applied to the

third terminal $V_{RF}=V_M \sin(\omega_S t)$. The output signal can be measured as the voltage over R_0. For each i-MTJ, the conductance G_i is given by $G_i=G_{<M>,i}+\Delta G_i \sin(\omega_i t+\phi_i)$ where $G_{<M>,i}$ is the average conductance, ΔG_i, ω_i and ϕ_i are, respectively, the amplitude, frequency and, the intrinsic phase shift of the oscillation generated in the i-MTJ. For N-synchronized MTJs at the frequency ω_S, the total conductivity is given by $G_T=\sum_{i=1...N} G_{<M>,i}+\sum_{i=1...N}\Delta G_i \sin(\omega_S t+\phi_i)$. The electrical circuit is completed by adding two filters with the aim to use the synchronization scheme to enhance the output microwave power at $2\omega_S$ or the dc voltage. In the case of pass-band filters, Z_0 and Z_1 are composed by a capacitor and an inductor connected in series, where $L_0C_0=\frac{1}{4\omega_S^2}$ and $L_1C_1=\frac{1}{\omega_S^2}$ respectively. In this way, the output voltage measured over R_0 is given by:

$$v_0=R_0 i_0=\frac{R_0 V_M}{2}\sum_{i=1...N}\Delta G_i \cos(2\omega_S t+\phi_i) \qquad (3)$$

When ϕ_i values are the same (or within a range smaller than 10 degree), v_0 can be approximated to the sum of the signals from the MTJs as $v_0 \approx 0.5 R_0 V_M \cos(2\omega_S t+\phi_S)\sum_{i=1...N}\Delta G_i$. If Z_0 is a low pass filter (i.e. a capacitor) and Z_1 is a high pass filter (i.e. an inductor), the output voltage over R_0 is given by:

$$v_0=-\frac{R_0 V_M}{2}\sum_{i=1...N}\Delta G_i \cos(\phi_i) \qquad (4)$$

The equations (3) and (4) point out how the proposed synchronization scheme can give rise to an improvement of the dynamical properties (for example power) if used as oscillator, or to an enhancement of the sensitivity (output dc voltage over the power of the microwave signal) when used as microwave detector.

IV. CONCUSIONS

In summary, we have micromagnetically studied the dynamical behavior of a three terminal MTJs driven by the SOT and the STT. We have found that the control of the STT and the SOT via electrically separated terminals opens promising perspective from a technological point of view in the design of next generation of spintronic oscillators and microwave detectors, overcoming the limit of the output power and sensitivity by means of an innovative highly scalable synchronization scheme.

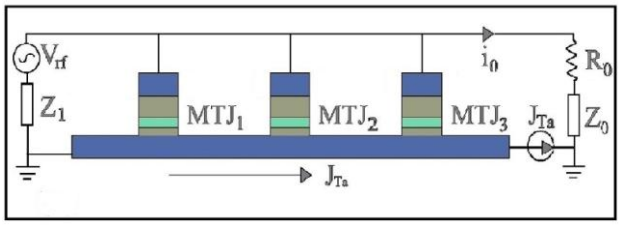

Fig. 4. (a) Schematic representation of the proposed highly scalable synchronization scheme.

REFERENCES

[1] F. Lamonaca, D. Grimaldi, R. Morello, IEEE Tran. on Instr. and Meas., (2014), in press. DOI 10.1109/TIM.2014.2299526

[2] G. Drenkow, Proc. of IEEE Autotestcon, pp. 100–105, (2006).

[3] F. Lamonaca, D. Grimaldi, , IEEE Transaction on Instrumentation and Measurement, Vol.62, Issue 2, pp. 38-49, (2013).

[4] M. Lipinski, T. Wlostowski, J. Serrano, and P. Alvarez, Proc. of IEEE ISPCS, pp. 25–30, (2011).

[5]F.Lamonaca, A.Gasparri, E.Garone, D.Grimaldi, IEEE Trans. on Instr. and Meas., (2014). DOI:10.1109/TIM.2014.2304867.

[6] I. M. Miron, K. Garello, G. Gaudin, P-J. Zermatten, M. V. Costache, S. Auffret, S. Bandiera, B. Rodmacq, A. Schuhl, and P. Gambardella, Nature 476, 189-193, (2011).

[7] S. Emori, U. Bauer, S.-M. Ahn, E. Martinez, G. S. D. Beach, Nat. Mat, 12, 611–616 (2013).

[8] V. E. Demidov, S. Urazhdin, H. Ulrichs, V. Tiberkevich, A. Slavin, D. Baither, G. Schmitz, S. O. Demokritov, Nat. Mat. 11, 1028–1031 (2012).

[9] K. Garello, I. M. Miron, C. O. Avci, F. Freimuth, Y. Mokrousov, S. Blugel, S. Auffret, O. Boulle, G. Gaudin, P. Gambardella, Nat. Nano. 8, 587–593 (2013).

[10] L. Liu, C-F. Pai, Y. Li, H. W. Tseng, D. C. Ralph, R. A. Buhrman, Science 336, 555-558 (2012).

[11] L. Liu, C-F. Pai, D. C. Ralph, and R. A. Buhrman, Phys. Rev. Lett. 109, 186602 (2012).

[12] L. Lopez-Diaz, D. Aurélio, L. Torres, E. Martinez, M. A. Hernadez-Lopez, J. Gomez, O.Alejos, M. Carpentieri, G. Finocchio, and G. Consolo, J. Phys. D: Appl. Phys., 45, 323001 (2012).

[13] G. Finocchio, M. Carpentieri, E. Martinez, and B. Azzerboni, Appl. Phys. Lett. 102, 212410 (2013).

[14] J.C. Slonczewski, Phys. Rev. B 71, 024411 (2005).

[15] J.C. Slonczewski, J.Z. Sun, J. Magn. Magn. Mater. 310, 169 (2007).

[16] M. Carpentieri, G. Finocchio, B. Azzerboni, L. Torres, Phys. Rev. B 82, 094434 (2010).
[17]G. Finocchio, M. Carpentieri, A. Giordano and B. Azzerboni, Phys. Rev. B 86, 014438 (2012).
[18] Y. Zhou, J. Persson, S. Bonetti, J. Åkerman, Appl. Phys. Lett. 92, 092505 (2008).